NORMAL CROSS-SECTIONAL ANATOMY OF THE FELINE THORAX AND ABDOMEN: COMPARISON OF COMPUTED TOMOGRAPHY AND CADAVER ANATOMY

VALERIE F. SAMII, DVM, DAVID S. BILLER, DVM, PHILIP D. KOBLIK, DVM, MS

Computed tomographic images of two adult domestic short-haired cats were obtained with a whole body scanner. Images of the thorax and abdomen were compared with cross-sectional anatomy cadaver specimens from the same two cats. Anatomic structures were first identified on the cadaver specimens with the aid of numerous anatomy texts and references and were then identified and labeled on the computed tomographic images. Results from this project provide an atlas of normal cross-sectional gross and CT anatomy of the feline thorax and abdomen that can be used in the interpretation of any cross-sectional imaging modality. *Veterinary Radiology & Ultrasound, Vol. 39, No. 6, 1998, pp 504–511.*

Key words: normal cross-sectional feline anatomy, computed tomography.

Introduction

IN THE PAST decade, there has been a steady increase in the feline pet population in the United States and in other countries. Coincident with the increasing popularity of feline pets, there has been a dramatic evolution of the specialty field of feline medicine. As this field develops, it becomes increasingly clear that cats are not the same thing as small dogs. In the past decade, there has also been a steady increase in the use of cross-sectional imaging techniques such as ultrasound (US), computed tomography (CT), and magnetic resonance imaging (MRI). These imaging modalities have revolutionized the ability to noninvasively explore the contents of body cavities.

Accurate interpretation of US, CT, or MRI studies of the thorax and abdomen requires a thorough knowledge of the regional cross-sectional anatomy. Normal human and canine cross-sectional anatomy of the body with correlative CT images are available.[1–6] Similar descriptions of the normal gross and CT cross-sectional anatomy of the thorax and abdomen of the cat remains to be published. The purpose of this paper is to provide an atlas of normal cross-sectional anatomy of the feline thorax and abdomen using CT images and transverse gross anatomic sections from two adult cats.

Materials and Methods

Two conditioned, mature domestic short-haired cats weighing between 3 and 5 kg were used for the study. The animals were anesthesized with Telazol* given intramuscularly. Following induction of general anesthesia, the animals were maintained in dorsal recumbency throughout the experiment. CT imaging was performed with a GE 9800-Quick scanner. A contiguous series of 5-mm thick transverse slices was obtained from the level of the manubrium to the level of the coxofemoral joints. Scans were performed after administration of intravenous iodinated contrast medium.† Window width and window level were adjusted to optimize image quality. Images were displayed on a television monitor during the procedure. Hard copy images were obtained with a matrix camera. Images were displayed so that the animal's right side was to the viewers[1] left and the animal's ventrum was displayed at the top of the image.

Immediately after CT imaging was completed, the animals were euthanized using a barbiturate overdose. The cadavers were placed in a freezer in the same dorsal recumbent position as they had been in for the CT study. Once completely frozen, the cadavers were removed from the freezer and sectioned in the transverse plane with an electric bandsaw. Sections were made from just cranial to the manubrium to the level of the ischiatic arch. Each section was approximately 1-cm thick. Slices for each animal were numbered, placed on trays and wrapped in plastic to prevent freezer burn and replaced in the freezer. Twenty-four hours later, the sections were removed from the freezer and photographed with the cranial surface of each section facing the camera. A set of cadaver sections were chosen in which all the regional anatomic structures could be seen with a mini-

From the Department of Surgical Sciences, School of Veterinary Medicine, University of Wisconsin-Madison, Madison, WI.

Address correspondence and reprint requests to Valerie F. Samii, DVM, Department of Surgical and Radiological Sciences, School of Veterinary Medicine, University of California, Davis, CA 95616.

Received December 5, 1995; accepted for publication October 15, 1997.

*Tiletamine HCl/Zolazepam HCl, Fort Dodge Laboratories, Fort Dodge, KS.

†Renovist II (diatrizoate meglumine and diatrizoate sodium injection USP), 2 mls/kg IV.

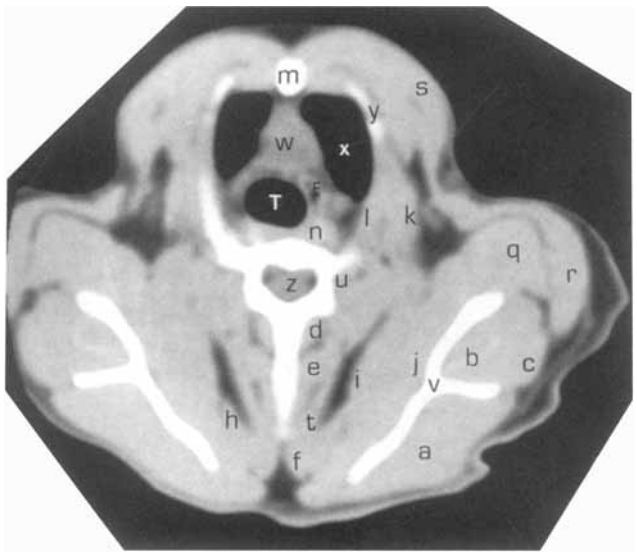

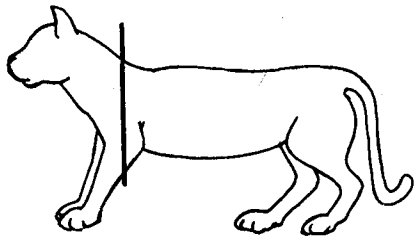

FIGURES 1 AND 2. a. supraspinatus m., b. infraspinatus m., c. deltoideus m., d. multifidus thoracis m., e. thoracic spinal m., f. rhomboideus m., g. trapezius m., h. splenius capitus m., i. serratus ventralis m. (cervicis and thoracis), j. subscapularis m., k. rectus thoracis m., l. intercostal mm., m. manubrium, n. longus colli m., o. brachiocephalic trunk, p. left and right axillary veins (Fig. 1 only), q. teres major m., r. triceps brachii m. (long head), s. pectoratis mm. (superficial and deep), t. semispinalis capitus m., u. complexus m., v. scapula, w. cranial vena cava, x. left cranial lung lobe, y. internal intercostal m., z. spinal cord, E. esophagus, T. trachea.

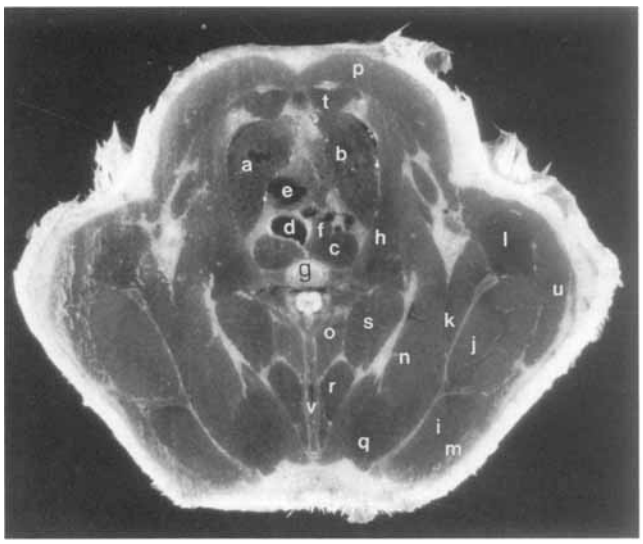

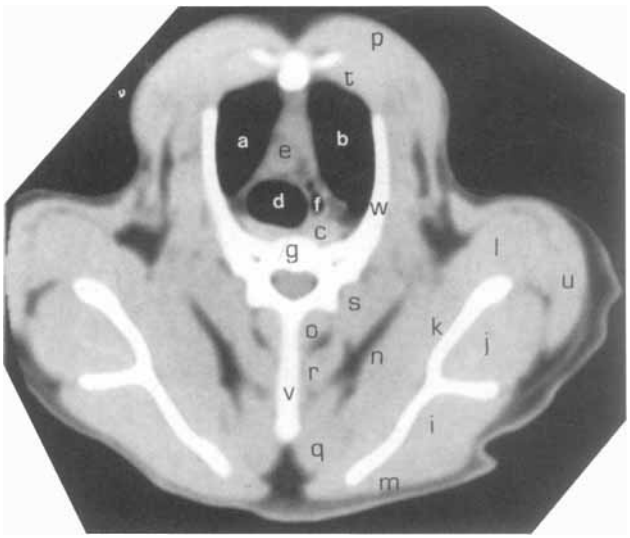

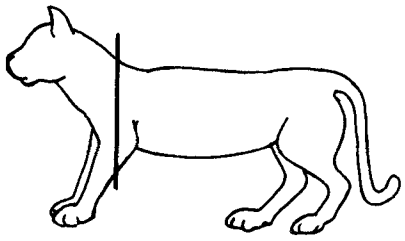

FIGURES 3 AND 4. a. right cranial lung lobe, b. left cranial lung lobe, c. longus colli m., d. trachea, e. cranial vena cava, f. esophagus, g. first thoracic vertebra, h. intercostal m. (Fig. 3 only), i. supraspinatus m., j. infraspinatus m., k. subscapularis m., l. triceps brachii m. (long head), m. trapezius m., n. serratus ventralis m. (cervicis and thoracis), o. multifidus thoracis m., p. deep pectoral m., q. rhomboideus thoracis m., r. spinalis et semispinalis thoracis et cervicis, s. longissimus thoracis m., t. transverse thoracis m., u. deltoideus m., v. spinous process of the first thoracic vertebra., w. left first rib (Fig. 4 only).

mum repetition of specific structures. Individual anatomic structures were first identified in photographic slides of the cadaver sections with the aid of multiple anatomic references.[3,5–9] Line drawings of these structures were produced from the photographic slides. CT slices were chosen that

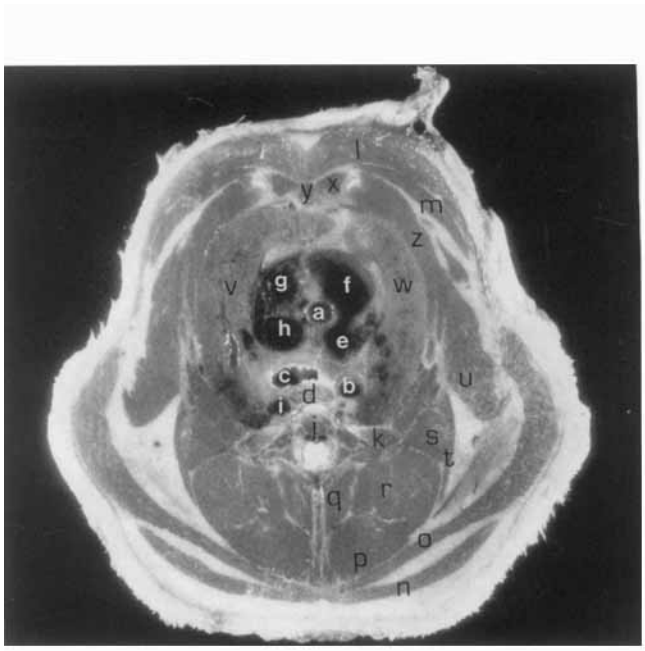

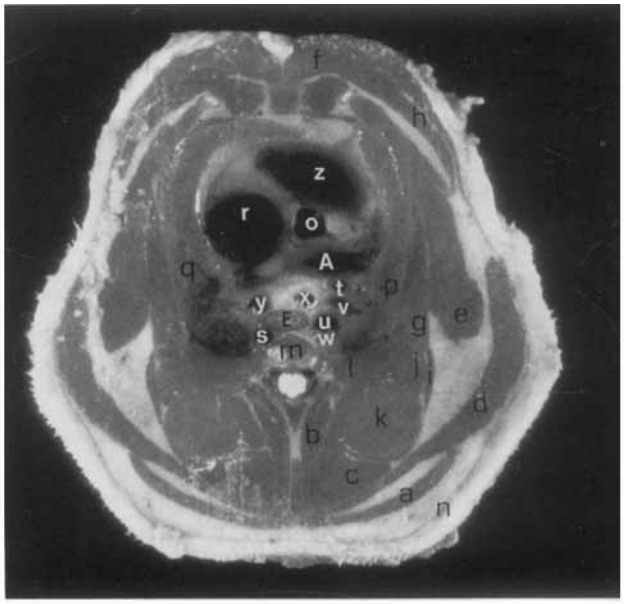

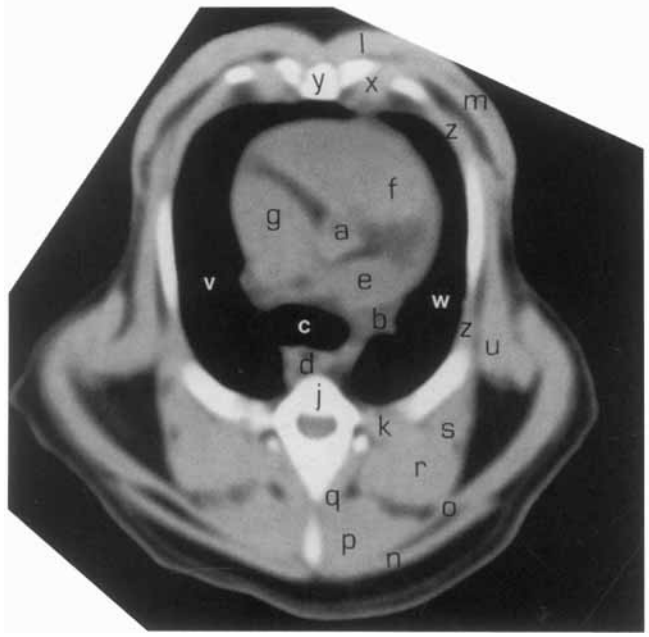

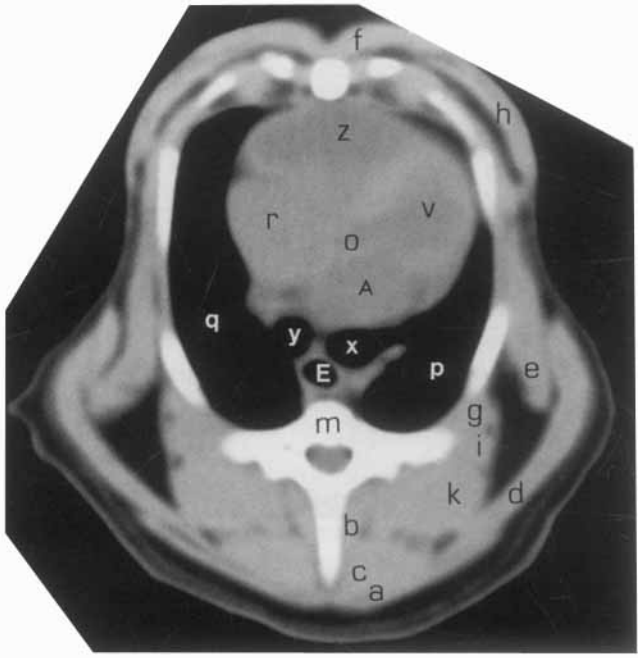

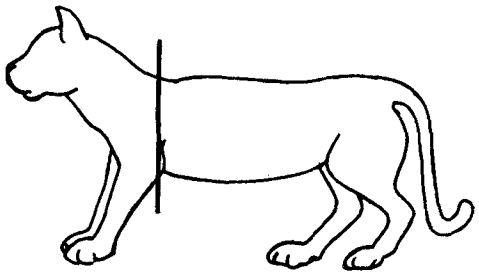

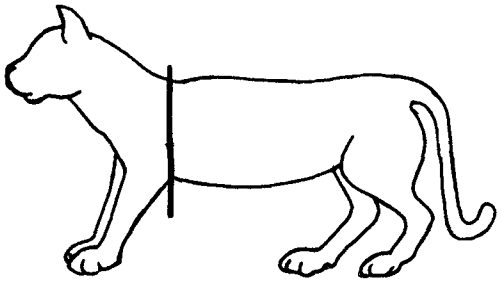

FIGURES 5 AND 6. a. ascending aorta, b. descending aorta, c. trachea, d. esophagus, e. pulmonary trunk, f. right ventricle, g. right atrium, h. right auricle (Fig. 5 only), i. azygous vein (Fig. 5 only), j. thoracic vertebra, k. longus colli m., l. deep (ascending) pectoral, m. rectus abdominis m., n. trapezius m., o. latissimus dorsi m., p. rhomboideus thoracic m., q. multifidus thoracis m., r. spinalis et semispinalis thoracis et cervicis m., s. thoracic iliocostal m., t. serratus dorsalis cranialis m. (Fig. 5 only), u. serratus ventralis m., v. right cranial lung lobe, w. left cranial lung lobe, x. internal intercostal m., y. sternebra, z. internal and external intercostal mm.

FIGURES 7 AND 8. a. trapezius m., b. multifidus thoracis m., c. spinalis et semispinalis thoracis et cervicis m., d. latissimus dorsi m., e. serratus ventralis m., f. deep ascending pectoral m., g. external intercostal m., h. rectus abdominis m., i. seratus dorsalis cranialis m., j. thoracic iliocostal m., k. longissimus thoracis m., l. rotator mm. (Fig. 7 only), m. thoracic vertebra, n. cutaneous trunci m. (Fig. 7 only), o. aortic ostium, p. left cranial lung lobe, q. right cranial lung lobe, r. right atrium, s. azygous vein (Fig. 7 only), t. left pulmonary vein (Fig. 7 only), u. aorta (Fig. 7 only), v. left pulmonary artery, w. thoracic duct (Fig. 7 only), x. left bronchus, y. right bronchus, z. right ventricle, A. left atrium, T. trachea, E. esophagus, V. left ventricle (Fig. 8 only).

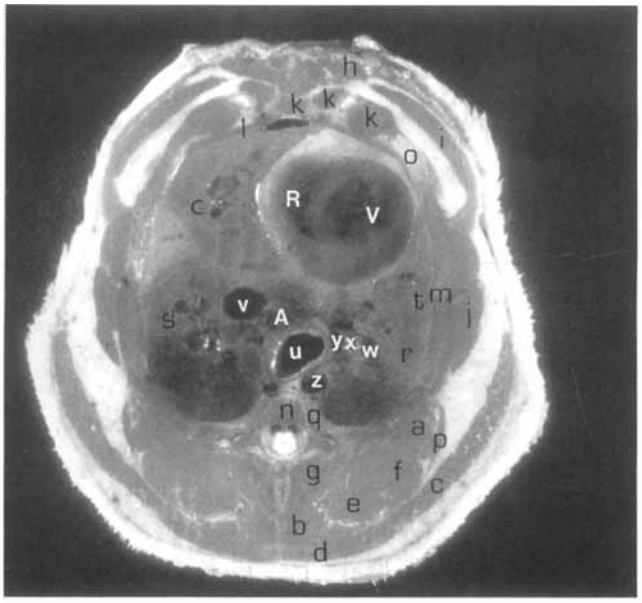

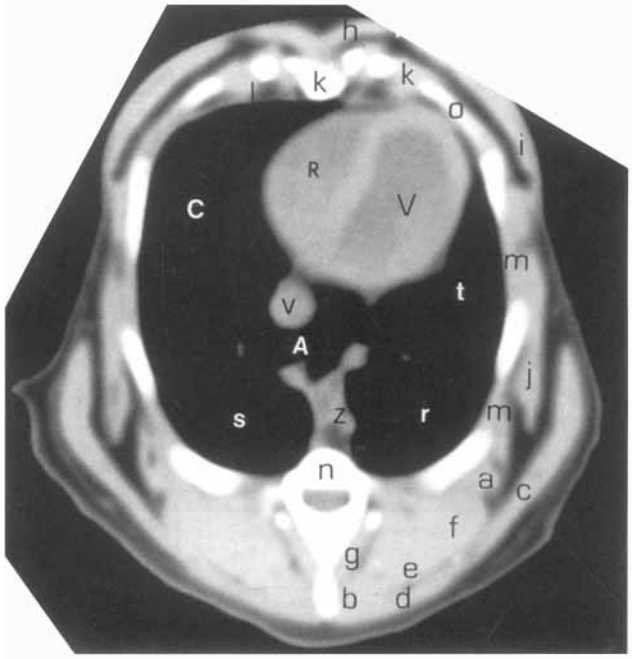

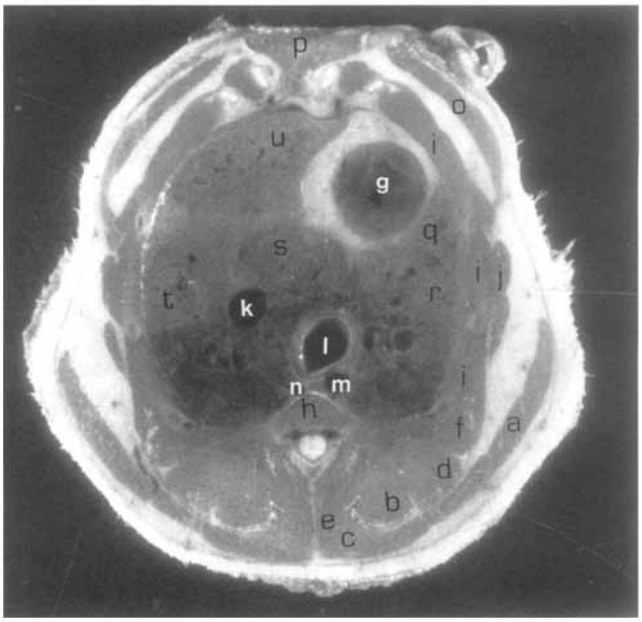

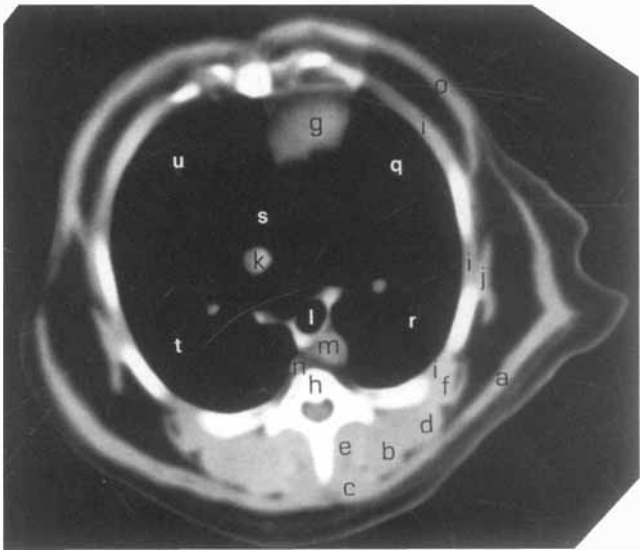

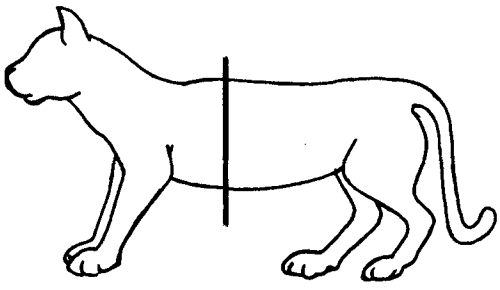

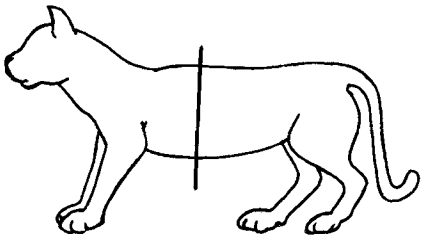

FIGURES 9 AND 10. a. iliocostalis thoracis m., b. rhomboideus thoracis m., c. latissimus dorsi m., d. trapezius m., e. spinalis et semispinalis thoracis et cervicis m., f. longissimus thoracis m., g. multifidus m., h. deep (ascending) pectoral m., i. rectus abdominis m., j. serratus ventralis m., k. sternum and intercostal mm., l. transversus thoracis m., m. internal and external intercostal mm., n. thoracic vertebra, o. costal cartilage, p. serratus dorsalis cranialis m. (Fig. 9 only), q. rotator mm. (Fig. 9 only), r. left caudal lung lobe, s. right middle and cranial lung lobes, t. caudal portion of left cranial lung lobe, u. esophagus (Fig. 9 only), v. caudal vena cava, w. left pulmonary artery (Fig. 9 only), x. left bronchus (Fig. 9 only), y. left pulmonary vein (Fig. 9 only), z. aorta. A. accessory lung lobe, C. right caudal lung lobe, R. right ventricle, V. left ventricle.

FIGURES 11 AND 12. a. latissimus dorsi m., b. spinalis et semispinalis thoracis et cervicis m., c. rhomboideus thoracis m., d. longissimus thoracis m., e. multifidus m., f. iliocostalis thoracis m., g. left ventricle, h. thoracic vertebra, i. internal and external intercostal mm., j. serratus ventralis m., k. caudal vena cava, l. esophagus, m. aorta, n. azygous vein, o. rectus abdominis m., p. deep (ascending) pectoral m. (Fig. 11 only), q. left cranial lung lobe, r. left caudal lung lobe, s. accessory lung lobe, t. right cranial and middle lung lobes, u. right caudal lung lobe.

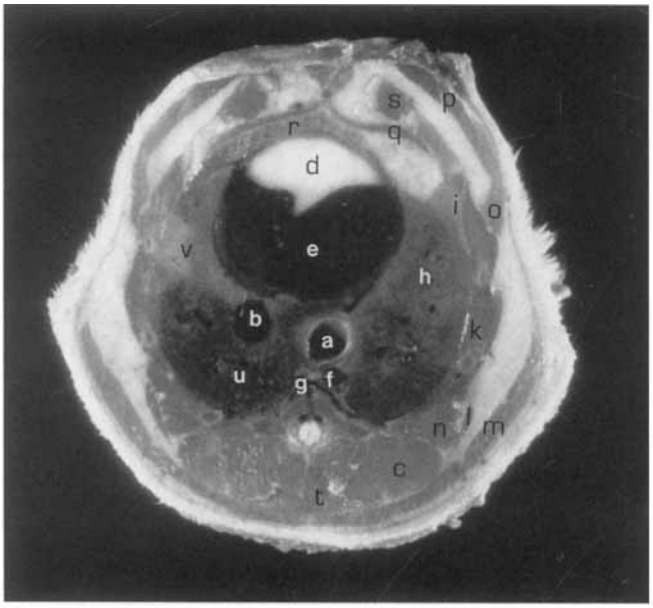

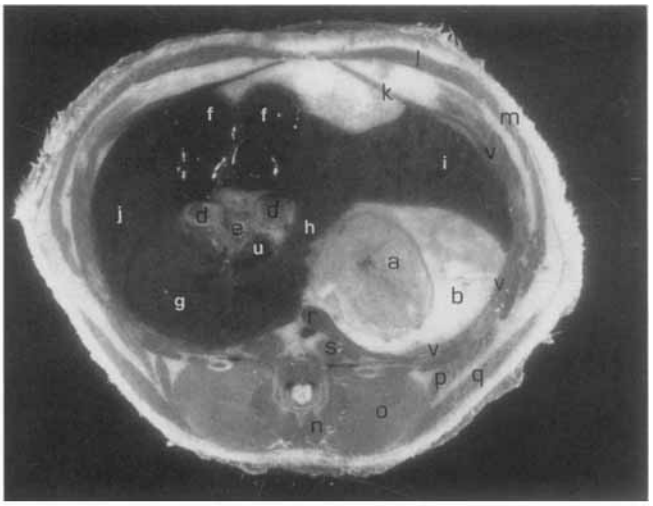

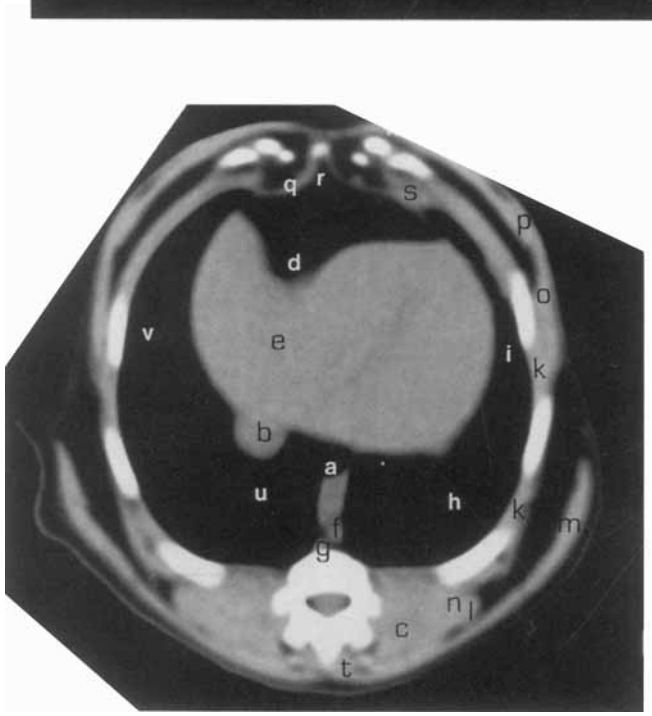

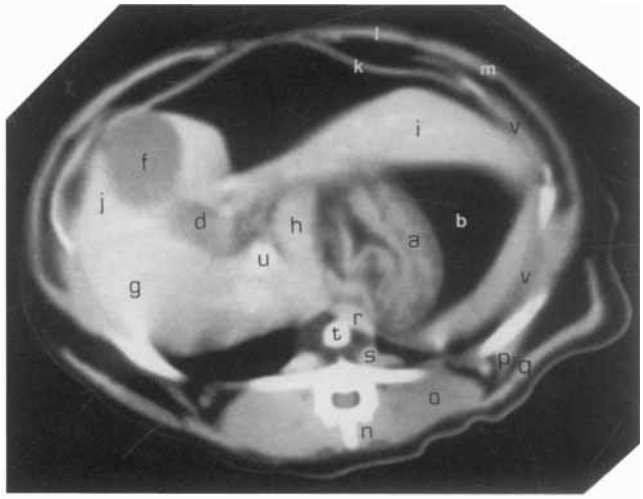

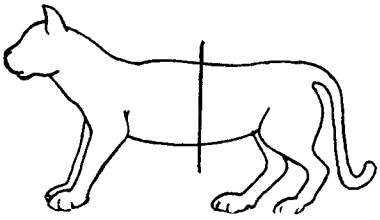

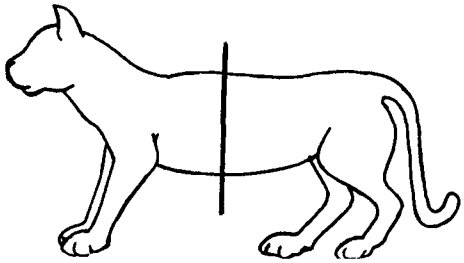

FIGURES 13 AND 14. a. esophagus, b. caudal vena cava, c. longissimus thoracis et lumborum m., d. falciform fat, e. liver, f. aorta, g. azygous vein, h. left caudal lung lobe, i. left lung lobe, k. internal and external intercostal mm., l. serratus dorsalis caudalis m., m. latissimus dorsi m., n. iliocostalis thoracis m., o. external abdominal oblique, p. rectus abdominis m., q. transversus abdominis m., r. middle right lung lobe, s. internal intercostal m., t. multifidus thoracis and multifidus lumborum mm., u. accessory lung lobe, v. right caudal lung lobe.

FIGURES 15 AND 16. a. stomach, b. omental fat, d. duodenum, e. pancreas (Fig. 15 only), f. gall bladder ("folded" when sectioned), g. caudate liver lobe, h. papillary process of liver, i. left lateral liver lobe, j. right lateral liver lobe, k. transversus abdominis m., l. rectus abdominis m., m. external abdominal oblique m., n. multifidus thoracis and multifidus lumborum mm., o. longissimus thoracis et lumborum m., p. serratus dorsalis caudalis m., q. latissimus dorsi m., r. crura of the diaphragm, s. psoas m., t. aorta, u. caudal vena cava and portal veins, v. internal and external intercostal mm.

most closely matched each cadaver section. Anatomic structures identified on the cadaver sections were then correlated to analogous structures on corresponding CT slices. Some structures found on the gross anatomic specimens could not be identified on the corresponding CT images and vice versa.

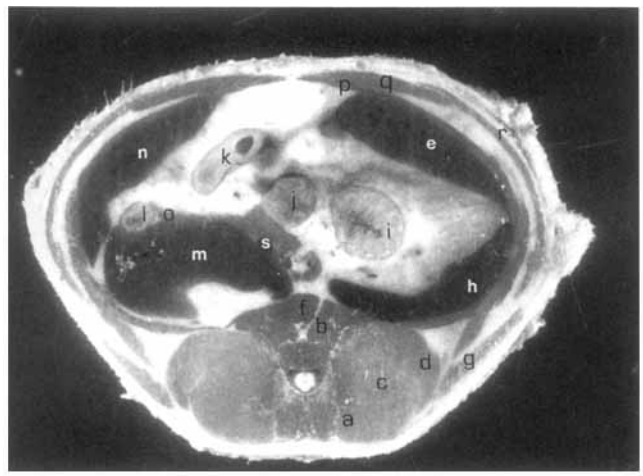

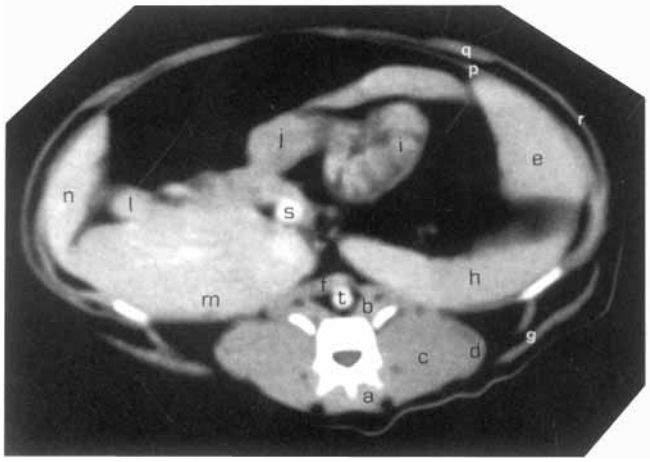

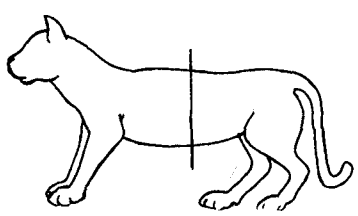

FIGURES 17 AND 18. a. multifidus lumborum m., b. psoas m., c. longissimus et lumborum m., d. iliocostalis et lumborum m., e. left lateral liver lobe, f. crura of the diaphragm, g. serratis dorsalis caudalis m., h. spleen, i. stomach, j. pylorus, k. jejunum, l. duodenum, m. caudate liver lobe, n. right lateral liver lobe, o. pancreatic, p. transversus abdominis m., q. rectus abdominis m., r. external abdominal oblique, s. caudal vena cava, t. aorta.

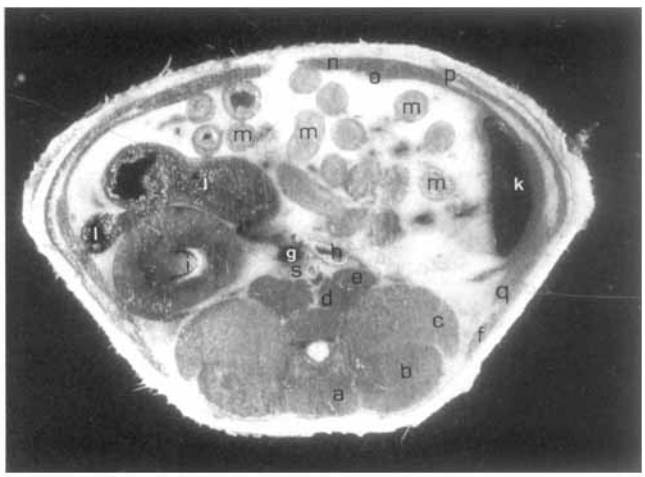

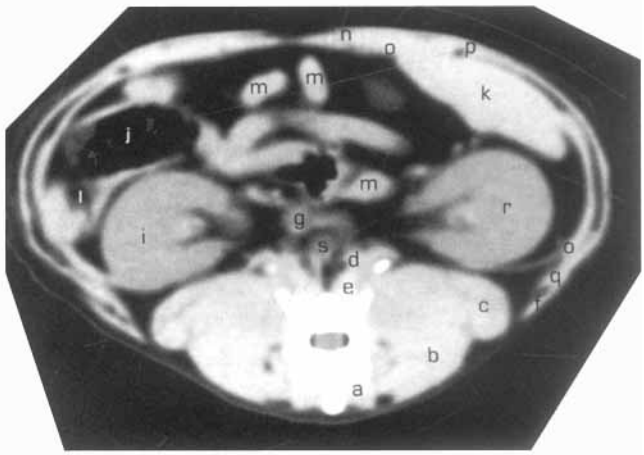

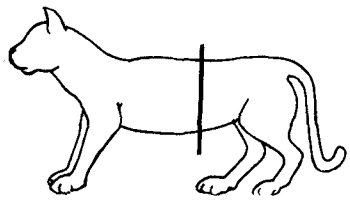

FIGURES 19 AND 20. a. multifidus lumborum m., b. longissimus et lumborum, c. iliocostalis et lumborum m., d. crura of the diaphragm, e. psoas m., f. serratis dorsalis caudalis m., g. caudal vena cava, h. left adrenal gland (Fig. 19 only), i. right kidney, j. transverse colon, k. spleen, l. cecum, m. jejunum, n. rectus abdominis m., o. transversus abdominis m., p. external abdominal oblique m., q. internal abdominal oblique m., r. left kidney, s. aorta.

Results

Twelve cadaver cross sections with their corresponding CT images and line drawings were selected. These sections are presented in a cranial-to-caudal progression from the level of the manubrium to approximately the level of the fourth lumbar vertebra. Identifiable anatomic structures were labeled on both the line drawings of the cadaver sections and on the corresponding CT images. Structures with bilateral symmetry were only labeled on one side.

Discussion

Our intent was to produce an atlas of cross-sectional anatomy of the feline abdomen and thorax that could be used as an aid in the interpretation of any cross-sectional imaging study. We were aware that black-and-white photographs of the cadaver sections would not provide high contrast images of many structures and elected to include CT images to improve the graphic display of the gross anatomy. We also felt that CT was a reasonable choice for a correlative imaging modality relative to US and MRI.

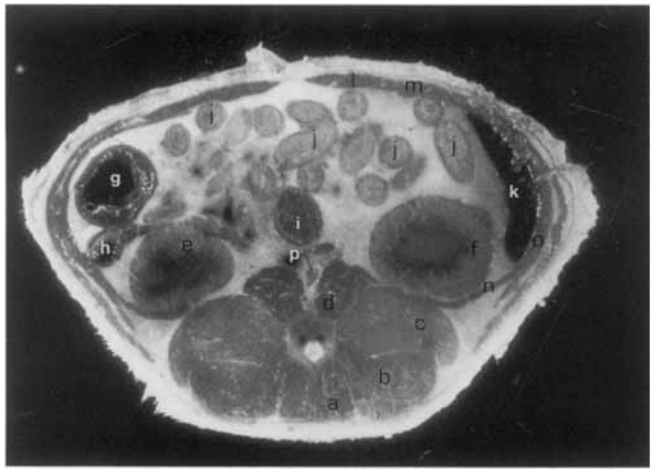

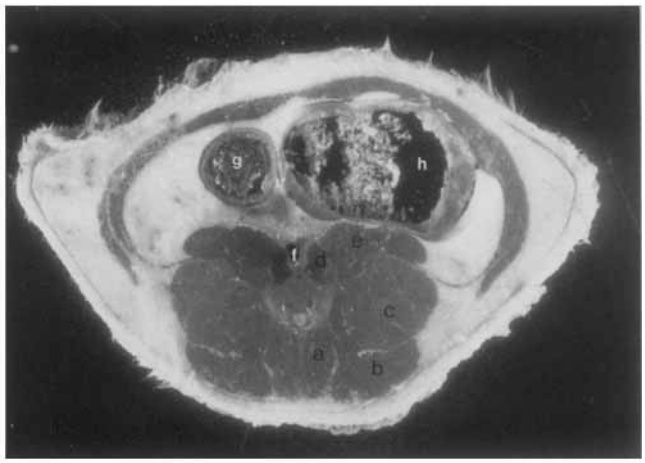

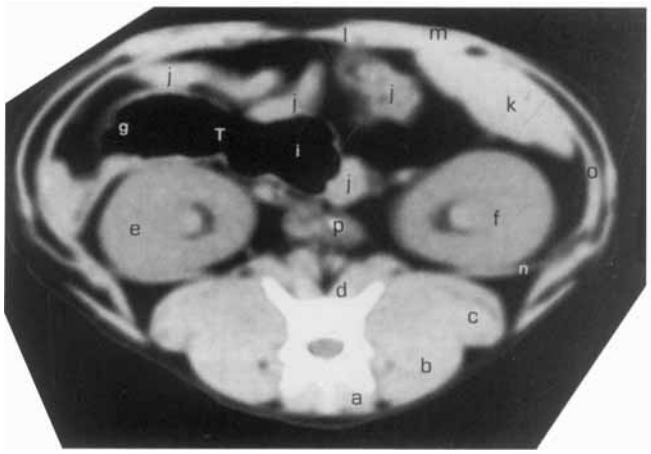

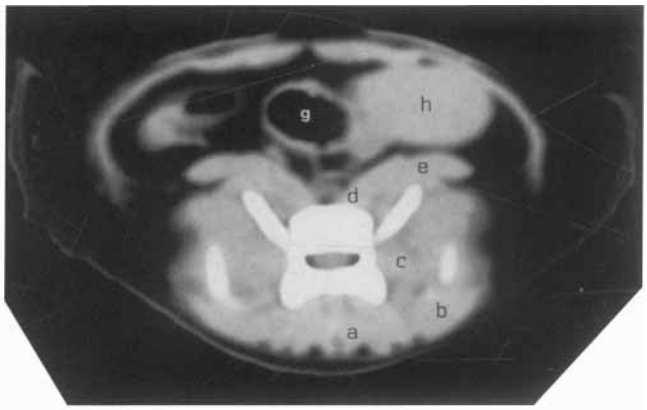

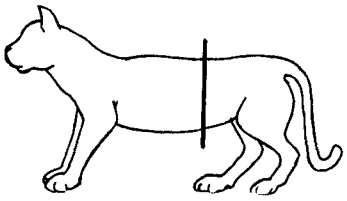

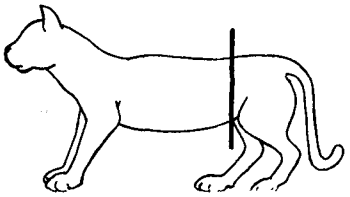

FIGURES 21 AND 22. a. multifidus lumborum m., b. longissimus et lumborum m., c. iliocostalis et lumborum m., d. psoas m., e. right kidney, f. left kidney, g. ascending colon, h. cecum (Fig. 21 only), i. descending colon, j. jejunum, k. spleen, l. rectus abdominis m., m. external abdominal oblique m., n. transversus abdominis m., o. internal abdominal oblique m., p. caudal vena cava, T. transverse colon (Fig. 22 only).

FIGURES 23 AND 24. a. multifidus lumborum m., b. longissimus et lumborum m., c. iliocostalis et lumborum m., d. psoas major m., e. quadratus lumborum m., f. caudal vena cava (Fig. 23 only), g. descending colon, h. urinary bladder.

Of the three imaging modalities, certainly US is the most available, particularly for examination of the abdominal cavity. There are several major limitations associated with US imaging that make it an unsatisfactory method to display cross-sectional anatomy. Individual ultrasound images represent only a portion of the complete cross-sectional anatomy for any given level of the body. Furthermore, the ultrasound beam is unable to penetrate structures that contain gas or mineral, further limiting the useful field of view in the abdomen, especially the thorax. Finally, compared with CT and MRI, US images have relatively poor resolution and soft tissue contrast.

Used equipment and tolerable service costs have allowed a slow, but steady, increase in the use of CT imaging in veterinary medicine. CT can produce high-detail images with good soft tissue contrast of the thorax and abdomen. Image quality is, however, adversely affected by patient motion and requires virtually all CT studies to be performed on anesthetized patients. In our experience, abdominal CT scans are usually requested to define the relationship of a known abdominal mass to adjacent vital structures better or to evaluate known or suspected lesions involving the axial spine and pelvic canal. CT images of the thorax are used to improve detection of subtle pulmonary lesions, to differentiate thoracic masses from accumulations of mediastinal or pleural fluid, and, again, to evaluate the caudal cervical and thoracic spine. MRI has many of the same advantages and

disadvantages of CT. MRI is capable of producing high-resolution/high-contrast cross-sectional images of the entire abdominal or thoracic cavity but requires that the patient be anesthetized for the imaging procedure. The high cost of equipment purchase and upkeep has limited the availability of MRI in veterinary medicine.

Our experience with attempting to train students in abdominal ultrasound indicates that lack of familiarity with the normal cross-sectional anatomy is a major factor slowing the learning process. We have also found that most students have a difficult time creating an accurate mental image of cross-sectional anatomy from pictures or line drawings used in most anatomy texts. The easiest way to learn cross-sectional anatomy is directly from cross-sectional images. The intent of this paper is to provide an atlas of the normal cross-sectional anatomy of the abdomen and thorax of the cat with the hope that it will promote the application of US, CT, and MRI in this species (Figs. 1–24).

REFERENCES

1. Wyman AC, Lawson TL, Goodman LR. Transverse anatomy of the human thorax, abdomen and pelvis. In: An atlas of anatomic radiologic computed tomographic and ultrasonic correlation. Boston: Little, Brown and Co, 1978.

2. Fike JR, Drury EM, Zook BC, et al. Canine anatomy as assessed by computed tomography. Am J Vet Res 1980;41:1823–1832.

3. Zook BC, Hitzelberg RA, Bradley EW. Cross-sectional anatomy of the beagle thorax. Vet Radiol 1989;30:277–281.

4. Feeney DA, Fletcher TF, Hardy RM. Atlas of correlative imaging anatomy of the normal dog: Ultrasound and computed tomography, 1st ed. Philadelphia: WB Saunders, 1991.

5. Smallwood JE, George TF. Anatomic atlas for computed tomography in the mesaticephalic dog: Thorax and cranial abdomen. Vet Radiol 1993;34:65–84.

6. Smallwood JE, George TF. Anatomic atlas for computed tomography in the mesaticephalic dog: Caudal abdomen and pelvis. Vet Radiol 1993;34:143–167.

7. Hudson LC, Hamilton WP. Atlas of feline anatomy for veterinarians, 1st ed. Philadelphia: WB Saunders, 1993.

8. Evans HE, Christensen GC. Miller's anatomy of the dog, 3rd ed. Philadelphia: WB Saunders, 1993.

9. Evans HE, deLahunta A. Miller's guide to dissection of the dog, 2nd ed. Philadelphia: WB Saunders, 1988.

10. Shively MJ. Veterinary anatomy: Basic, comparative, and clinical, College Station, TX: Texas A & M University Press, 1984.

11. Popesko P. Atlas of topographical anatomy of the domestic animals, vol 1, 2nd ed. Philadelphia, WB Saunders, 1975.